J|A|C|S ARTICLES

Published on Web 01/27/2010

Unusual Relaxation Pathway from the Two-Photon Excited First Singlet State of Carotenoids

Yoonsoo Pang, Garth A. Jones, Matthew A. Prantil,† and Graham R. Fleming*

Department of Chemistry, University of California, Berkeley, and Physical Biosciences Division, Lawrence Berkeley National Laboratory, Berkeley, California 94720-1460

Received October 5, 2009; E-mail: GRFleming@lbl.gov

Abstract: Transient infrared and visible absorption measurements along with density functional theory (DFT) calculations on carotenoids 8′-apo-β-caroten-8′-al (**I**) and 7′,7′-dicyano-7′-apo-β-carotene (**II**) were used to explore the nature of a long-lived species observed in transient infrared absorption measurements following two-photon excitation (Pang et al. *J. Phys. Chem. B* **2009**, *113*, 13806). The long-lived species of **I** has a very strong infrared absorption around 1510 cm^{-1} and a visible transient absorption band centered at 760 nm. The long-lived species appears on two different time scales of ~16 and 140−270 ps. The longer rise component is absent in nonpolar solvents. DFT calculations using the B3LYP functional and the 6-31G(d) basis set were used to investigate the ground-state potential-energy surface of **I** and **II** including its conformational isomers, a π-diradical "kinked" structure, and cation and neutral radicals. From the simulated infrared spectra of all the structures considered, we found a close match in the cation radical spectrum to the experimental infrared spectrum of the long-lived species. However, the visible absorption band does not match that of the monomeric cation radical. On the basis of our experimental and theoretical results, we propose a charge-transfer complex between a carotenoid and a solvent molecule for the origin of the long-lived species formed from the direct two-photon excitation of the S_1 state.

Introduction

Carotenoids are naturally occurring pigment molecules found in the chloroplasts of plants and in photosynthetically active organisms such as algae and bacteria. In higher plants, carotenoids are principally involved in light harvesting[1,2] and photoprotection.[3,4] Carotenoids may play a role in human disease prevention by scavenging free radicals.[5] A full understanding of the role of carotenoids in a wide range of natural optically initiated processes requires an understanding of both ground- and excited-state potential surfaces and the dynamics associated with the excited states. Numerous theoretical and experimental studies have demonstrated that the excited-state behavior of carotenoid molecules is exceedingly complex, a fact that doubtless underpins their broad range of applications in nature.[6]

The excited-state structure of carotenoids is generally described by reference to the C_{2h} geometry of simple all-*trans*-polyenes.[1,7] This leads to a simplified energy level scheme, composed of the lower singlet excited states, S_2 ($1B_u^+$) and S_1 ($2A_g^-$), and the ground state, S_0 ($1A_g^-$). The electronic structure of carotenoids has proved enormously challenging to calculate, and to date a full exploration of the excited-state potential surfaces at an adequate level of theory has not been possible. As we noted in refs 8 and 9, two recent publications find rather different results for the change in bond length alternation in S_2 with respect to S_0. Recent studies successfully used density functional theory (DFT) methods to describe the ground-state electronic structure and the vibrational spectra of several important carotenoids.[8,10−15] Fleming, Head-Gordon, and coworkers first used time-dependent DFT (TD-DFT) to study the excited states of carotenoids and energy transfer between carotenoids and chlorophylls in light-harvesting complexes.[10,16] The excited-state structures of carotenoids violaxanthin, zeax-

† Current address: Lawrence Livermore National Laboratory, P.O. Box 808, Livermore, CA 94551-0808.

(1) Frank, H. A.; Cogdell, R. J. *Photochem. Photobiol.* **1996**, *63*, 257.
(2) (a) van Amerongen, H.; van Grondelle, R. *J. Phys. Chem. B* **2001**, *105*, 604. (b) Ritz, T.; Damjanovic, A.; Schulten, K.; Zhang, J. P.; Koyama, Y. *Photosynth. Res.* **2000**, *66*, 125.
(3) (a) Niyogi, K. K. *Annu. Rev. Plant Physiol. Plant Mol. Biol.* **1999**, *50*, 333. (b) Demmig-Adams, B.; Adams, W. W. *Science* **2002**, *298*, 2149.
(4) Holt, N. E.; Zigmantas, D.; Valkunas, L.; Li, X. P.; Niyogi, K. K.; Fleming, G. R. *Science* **2005**, *307*, 433.
(5) (a) El-Agamey, A.; Lowe, G. M.; McGarvey, D. J.; Mortensen, A.; Phillip, D. M.; Truscott, T. G.; Young, A. J. *Arch. Biochem. Biophys.* **2004**, *430*, 37. (b) Edge, R.; McGarvey, D. J.; Truscott, T. G. *J. Photochem. Photobiol., B* **1997**, *41*, 189.
(6) (a) Polívka, T.; Sundström, V. *Chem. Rev.* **2004**, *104*, 2021. (b) Polivka, T.; Sundstrom, V. *Chem. Phys. Lett.* **2009**, *477*, 1.
(7) Orlandi, G.; Zerbetto, F.; Zgierski, M. Z. *Chem. Rev.* **1991**, *91*, 867.
(8) Dreuw, A. *J. Phys. Chem. A* **2006**, *110*, 4592.
(9) Kleinschmidt, M.; Marian, C. M.; Waletzke, M.; Grimme, S. *J. Chem. Phys.* **2009**, *130*, 044708.
(10) (a) Hsu, C. P.; Walla, P. J.; Head-Gordon, M.; Fleming, G. R. *J. Phys. Chem. B* **2001**, *105*, 11016. (b) Vaswani, H. M.; Hsu, C. P.; Head-Gordon, M.; Fleming, G. R. *J. Phys. Chem. B* **2003**, *107*, 7940.
(11) Schlucker, S.; Szeghalmi, A.; Schmitt, M.; Popp, J.; Kiefer, W. *J. Raman Spectrosc.* **2003**, *34*, 413.
(12) Liu, W. L.; Wang, Z. G.; Zheng, Z. R.; Li, A. H.; Su, W. H. *J. Phys. Chem. A* **2008**, *112*, 10580.
(13) Requena, A.; Ceron-Carrasco, J. P.; Bastida, A.; Zuniga, J.; Miguel, B. *J. Phys. Chem. A* **2008**, *112*, 4815.
(14) Durbeej, B.; Eriksson, L. A. *Phys. Chem. Chem. Phys.* **2004**, *6*, 4190.
(15) Wirtz, A. C.; van Hemert, M. C.; Lugtenburg, J.; Frank, H. A.; Groenen, E. J. J. *Biophys. J.* **2007**, *93*, 981.
(16) Walla, P. J.; Linden, P. A.; Hsu, C. P.; Scholes, G. D.; Fleming, G. R. *Proc. Natl. Acad. Sci. U.S.A.* **2000**, *97*, 10808.

10.1021/ja908472y

anthin, and lutein were explored in detail by TD-DFT,[8] and the molecular geometry and vibrational spectrum of β-carotene in the electronic ground state were also recently studied.[11,12]

It is well known that carotenoids are susceptible to oxidization, and there have been numerous experimental studies demonstrating radical formation in carotenoids in solution or in photosynthetic complexes.[4,17−19] The radical cation of carotenoids can be prepared in multiple ways: chemically by reaction with oxidizing agents, electrochemically under a positive voltammetric potential, and photochemically. Spectroscopic evidence for a carotenoid radical is provided by a strong $D_0 \rightarrow D_2$ absorption band in the near-infrared region at 800−1100 nm,[20−22] and the steady-state absorption spectra of many xanthophyll carotenoids were recently reported with a comprehensive set of references by Frank and co-workers.[19] Vibrational (infrared and resonance Raman) spectra of carotenoid radical cations in photosystem II and in solution have been reported,[23,24] and provide characteristic vibrational frequencies of cation radicals. Kispert and co-workers extensively studied carotenoid radicals by chemical and electrochemical oxidations,[20,23,25−28] and oxidation potentials of carotenoid 8′-apo-β-caroten-8′-al (**I**) and 7′,7′-dicyano-7′-apo-β-carotene (**II**) were reported as 900[28] and 739 mV[26] vs SCE and λ_{max} for the $D_0 \rightarrow D_2$ absorption band for both carotenoids as 845 nm.[23,28]

In our previous study,[29] we showed the existence of multiple minima on the S_1 potential-energy surface of carotenoids **I** and **II** by transient infrared absorption measurements. When the higher S_2 state is populated by one-photon excitation (1PE), a very fast (∼100 fs) internal conversion from the S_2 state populates the lower S_1 state. In this case the S_1 state decays to the ground state with a 0.5−30 ps time constant, depending on the conjugation length and solvent polarity. The one-photon forbidden S_1 state can also be directly populated by two-photon excitation (2PE) with near-infrared light,[16,30] but the excited-state dynamics of the S_1 state populated by 2PE are distinct from the 1PE case. Long-lived absorption bands appear subsequent to 2PE, but not 1PE, and are proposed to originate from a second minimum on the S_1 potential surface, which does not communicate with the minimum populated via S_2, and may be one of the conformational isomers proposed by Sundström and co-workers.[31]

In this study, we focus on the nature of the long-lived absorption bands of **I** and **II** observed in the 2PE transient infrared measurements. Transient absorption experiments and DFT simulations are used to explore the origin of this long-lived species.

Methods

The details of the laser setup have been given elsewhere.[29,32] Briefly, mid-infrared probe pulses (∼100 fs, 1250−3000 cm^{-1}) were generated by difference frequency generation in a $AgGaS_2$ crystal between the signal and the idler pulses of a near-infrared optical parametric amplifier (OPA). The near-infrared pump (∼60 fs, 1150−1500 nm) for 2PE was generated from another near-infrared OPA, and pulse energies at the sample position were kept at 5 μJ for both 1275 and 1400 nm pump. The OPAs were pumped by a fundamental pulse at 800 nm (∼35 fs, 1 mJ) produced by a Ti: sapphire amplifier system (Coherent Legend Elite USP). Midinfrared pulses were split into signal and reference and detected by two arrays of 32-element HgCdTe detector (Infrared Systems). Transient infrared spectra were measured at several center frequencies with a resolution of 2−4 cm^{-1} per pixel and stitched together to construct each spectrum over the 1350−1800 cm^{-1} range.

In the electronic probe experiments, visible pulses from a Coherent 9450 OPA or a white light generated from a sapphire window were used as the probe. Probe pulses were spectrally resolved in a double-grating monochromator with a 2 nm spectral bandwidth (DH10, Horiba Jobin Yvon) and detected by a silicon photodiode.

8′-Apo-β-caroten-8′-al (**I**) and all the solvents were purchased from Sigma-Aldrich, and 7′,7′-dicyano-7′-apo-β-carotene (**II**) synthesized from **I** was a gift from Kispert group.[33] Samples were used without further purification, concentrations of **I** and **II** solutions were varied from 0.5 to 2 g/L for infrared absorption measurements, and an order of magnitude more dilute solutions were used for the electronic probe measurements. A liquid cell with 200−250 μm thickness and a peristaltic pump were used for recirculating the sample.

For the DFT analysis of the ground-state carotenoid molecules, we used the Gaussian03 software package,[34] and the Gaussview 4.1 software is used to visualize the vibrational modes. The B3LYP functional and the 6-31G(d) basis set[13] were used to analyze the ground-state potential-energy surfaces of **I** and **II** including conformational isomers around C−C and C═C bonds within the polyene backbone and to simulate IR spectra from harmonic frequency analysis.

The potential-energy surface about a particular torsional degree of freedom is obtained by freezing a certain degree of freedom such as a torsional angle at a series of values (ranging from −180° to 180°) and by optimizing all the remaining degrees of freedom. Generally, the closed-shell structure calculations were performed using restricted wave functions, and the open-shell structures are optimized using unrestricted wave functions. However, in the case of the "kinked" diradical system, we used unrestricted wave functions in combination with the Gaussian03 input keyword of "GUESS = (MIX, ALWAYS)". This keyword forces the HOMO

(17) (a) Tracewell, C. A.; Vrettos, J. S.; Bautista, J. A.; Frank, H. A.; Brudvig, G. W. *Arch. Biochem. Biophys.* **2001**, *385*, 61. (b) El-Agamey, A.; McGarvey, D. J. *Carotenoids* **2008**, *4*, 119.
(18) (a) Han, R. M.; Tian, Y. X.; Wu, Y. S.; Wang, P.; Ai, X. C.; Zhang, J. P.; Skibsted, L. H. *Photochem. Photobiol.* **2006**, *82*, 538. (b) Han, R. M.; Wu, Y. S.; Feng, J.; Ai, X. C.; Zhang, J. P.; Skibsted, L. H. *Photochem. Photobiol.* **2004**, *80*, 326.
(19) Galinato, M. G. I.; Niedzwiedzki, D.; Deal, C.; Birge, R. R.; Frank, H. A. *Photosynth. Res.* **2007**, *94*, 67.
(20) Gao, Y. L.; Kispert, L. D. *J. Phys. Chem. B* **2003**, *107*, 5333.
(21) Zhang, J. P.; Fujii, R.; Koyama, Y.; Rondonuwu, F. S.; Watanabe, Y.; Mortensen, A.; Skibsted, L. H. *Chem. Phys. Lett.* **2001**, *348*, 235.
(22) Gurzadyan, G. G.; Steenken, S. *Phys. Chem. Chem. Phys.* **2002**, *4*, 2983.
(23) Jeevarajan, A. S.; Kispert, L. D.; Chumanov, G.; Zhou, C.; Cotton, T. M. *Chem. Phys. Lett.* **1996**, *259*, 515.
(24) (a) Vrettos, J. S.; Stewart, D. H.; de Paula, J. C.; Brudvig, G. W. *J. Phys. Chem. B* **1999**, *103*, 6403. (b) Telfer, A.; Frolov, D.; Barber, J.; Robert, B.; Pascal, A. *Biochemistry* **2003**, *42*, 1008. (c) Noguchi, T.; Mitsuka, T.; Inoue, Y. *FEBS Lett.* **1994**, *356*, 179.
(25) (a) Gao, Y. L.; Konovalova, T. A.; Xu, T.; Kispert, L. A. *J. Phys. Chem. B* **2002**, *106*, 10808. (b) Khaled, M.; Hadjipetrou, A.; Kispert, L. D. *J. Phys. Chem.* **1991**, *95*, 2438. (c) Ding, R.; Grant, J. L.; Metzger, R. M.; Kispert, L. D. *J. Phys. Chem.* **1988**, *92*, 4600.
(26) Jeevarajan, J. A.; Kispert, L. D. *J. Electroanal. Chem.* **1996**, *411*, 57.
(27) Gao, Y. L.; Focsan, A. L.; Kispert, L. D.; Dixon, D. A. *J. Phys. Chem. B* **2006**, *110*, 24750.
(28) Grant, J. L.; Kramer, V. J.; Ding, R.; Kispert, L. D. *J. Am. Chem. Soc.* **1988**, *110*, 2151.
(29) Pang, Y.; Prantil, M. A.; Van Tassle, A. J.; Jones, G. A.; Fleming, G. R. *J. Phys. Chem. B* **2009**, *113*, 13086.
(30) Walla, P. J.; Yom, J.; Krueger, B. P.; Fleming, G. R. *J. Phys. Chem. B* **2000**, *104*, 4799.
(31) Polívka, T.; Zigmantas, D.; Frank, H. A.; Bautista, J. A.; Herek, J. L.; Koyama, Y.; Fujii, R.; Sundstrom, V. *J. Phys. Chem. B* **2001**, *105*, 1072.
(32) Van Tassle, A. J.; Prantil, M. A.; Fleming, G. R. *J. Phys. Chem. B* **2006**, *110*, 18989.
(33) Oneil, M. P.; Wasielewski, M. R.; Khaled, M. M.; Kispert, L. D. *J. Chem. Phys.* **1991**, *95*, 7212.
(34) Frisch, M. J.; et al. *Gaussian 03*, Revision D.01; Gaussian, Inc.: Wallingford, CT, 2004.

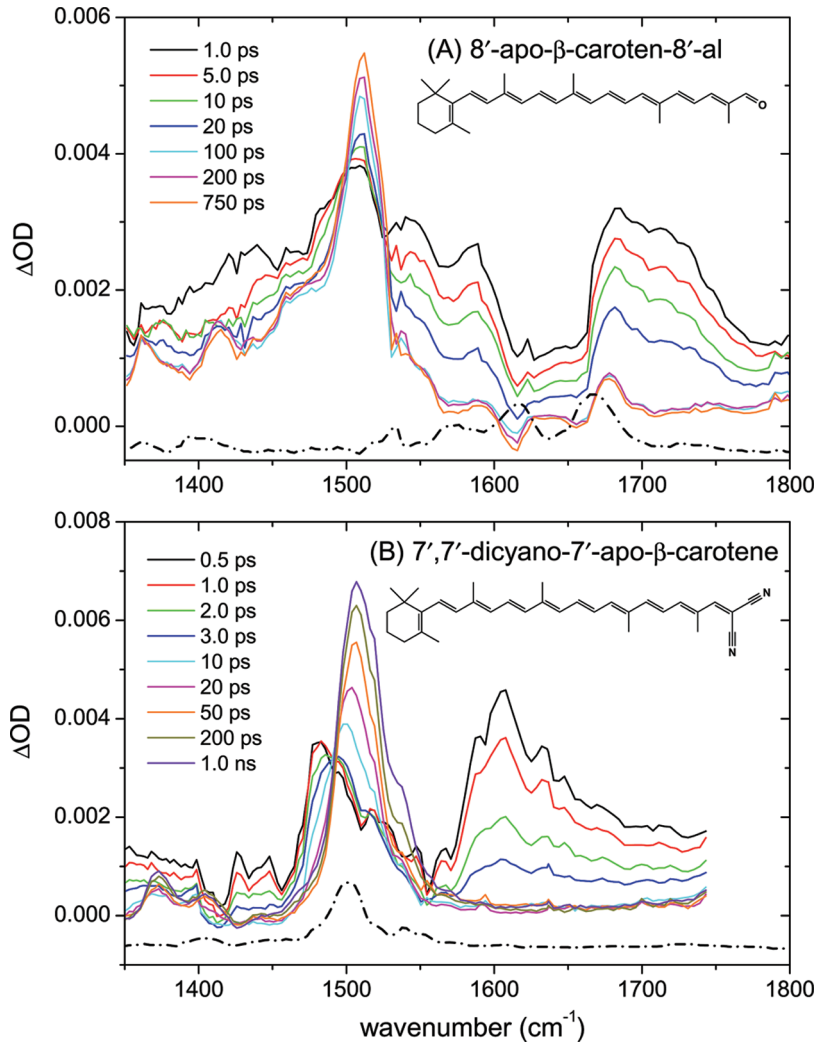

Figure 1. Transient infrared absorption spectra of (A) **I** and (B) **II** in chloroform solution following 2PE of 1275 and 1400 nm, respectively. The ground-state infrared spectra of both carotenoids in chloroform solution measured using the same spectrometer as that used in the transient measurements are shown as dash−dot lines, and molecular structures of both carotenoids are shown in the insets.

and LUMO to be mixed so as to destroy $\alpha-\beta$ and spatial symmetries of the "kinked" system. This allows one to optimize an unrestricted singlet state, producing a molecule with diradical character.

Results

Transient Infrared Absorption Measurements with Two-Photon Excitation (2PE). Figure 1 shows transient infrared absorption spectra at selected time delays of **I** and **II** in chloroform following 2PE of 1275 and 1400 nm, respectively. The infrared spectra of **I** before and after 100 ps are quite different with the appearance at longer time delays of a very intense peak at 1510 cm^{-1} along with other peaks at 1360, 1415, and 1678 cm^{-1} and a ground-state bleach at 1614 cm^{-1}. The spectrum of **II** completely changes around 5 ps delay with the appearance of a dominating 1507 cm^{-1} peak along with a few peaks at 1316 (not shown), 1373, and 1405 cm^{-1}. These long-lived absorption bands for **I** and **II** increase in amplitude over time and do not show decays on a 1 ns time scale.

Kinetic traces of the strong long-lived absorption bands around 1510 cm^{-1} for **I** and **II** in several solvents are shown in Figure 2 with fits to sums of exponentials. The long-lived absorption bands of **I** show different dynamics between polar (CD_3CN and $CHCl_3$) and nonpolar solvents (CCl_4). The band at 1515 cm^{-1} in CD_3CN shows a 147 ps rise component, and the band at 1510 cm^{-1} in $CHCl_3$ shows 15.4 and 142 ps rise components. This band does not show any decay on the 1 ns time scale in polar solvents. However, this band at 1508 cm^{-1} in CCl_4 shows a 16.8 ps rise then decays with ~342 ps lifetime. The lifetime of the S_1 state is solvent dependent as a result of intramolecular charge transfer[35] and slightly different between 1PE and 2PE. The S_1 lifetimes of **I** are 8.7 ps in CD_3CN, 19.4 ps in $CHCl_3$, and 29.2 ps in CCl_4 solution in 1PE infrared measurements, which increases with the decrease of solvent polarity. The S_1 lifetimes of **I** measured with 2PE were a little shorter than 1PE values in polar solvents (7.4 ps in CD_3CN and 17.2 ps in $CHCl_3$) but almost identical in nonpolar solvent (30.8 ps in CCl_4). It is also notable that the frequency of the strong long-lived absorption band of **I** blue shifts from 1508 to 1515 cm^{-1} as the solvent polarity increases.

The long-lived absorption band of **II** at 1507 cm^{-1} shows 16.5 and 233 ps rise components with no decay in 1 ns. The S_1 lifetime of carotenoid **II** was measured as 2.0 ps with 1PE and

(35) (a) He, Z. F.; Gosztola, D.; Deng, Y.; Gao, G. Q.; Wasielewski, M. R.; Kispert, L. D. *J. Phys. Chem. B* **2000**, *104*, 6668. (b) Ehlers, F.; Wild, D. A.; Lenzer, T.; Oum, K. *J. Phys. Chem. A* **2007**, *111*, 2257.

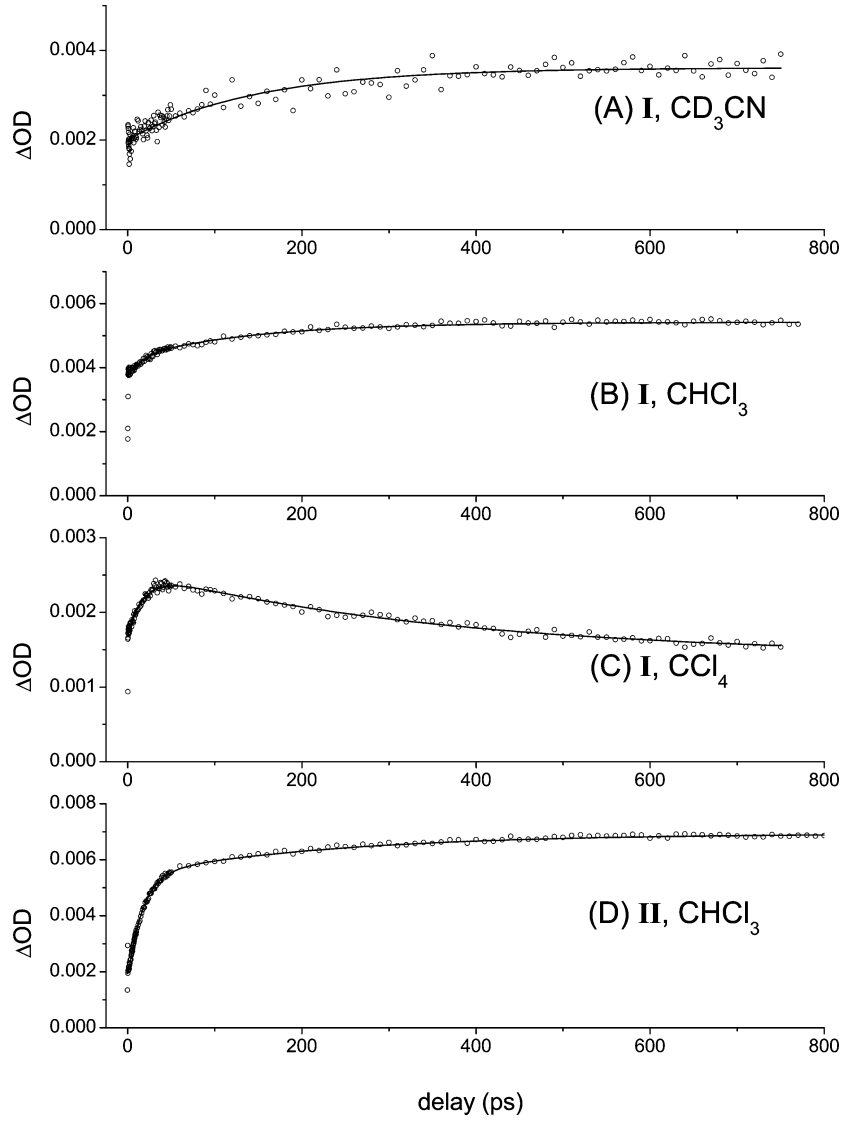

Figure 2. Kinetic traces (circles) and exponential fits (lines) for long-lived absorption bands around 1510 cm^{-1} in the transient infrared absorption spectra of **I** in (A) CD_3CN, (B) $CHCl_3$, and (C) CCl_4 solution and **II** in (D) $CHCl_3$ solution for 2PE.

Table 1. Dynamics of the S_1 State and Long-Lived Absorption Band for 8′-Apo-β-caroten-8′-al and 7′,7′-Dicyano-7′-apo-β-carotene[a,b]

λ_{ex}[c] (nm)	solvent	τ_{S1} (ps)	a_1[d]	τ_1 (ps)	a_2[d]	τ_2 (ps)
		8′-Apo-β-caroten-8′-al (**I**)				
490 (1PE)	CD_3CN	8.7 ± 0.1				
	$CHCl_3$	19.4 ± 0.2				
	CCl_4	29.2 ± 0.5				
1275 (2PE)	CD_3CN	7.4 ± 0.8			−1.00	147 ± 13
	$CHCl_3$	17.2 ± 0.4	−0.33	15.4 ± 2.4	−0.67	142 ± 9
	CCl_4	30.8 ± 1.8	−0.72	16.8 ± 0.9	1.00	342 ± 24
		7′,7′-Dicyano-7′-apo-β-carotene (**II**)				
508 (1PE)	CD_3CN	0.50 ± 0.01				
	$CHCl_3$	2.0 ± 0.1				
	CCl_4	9.1 ± 0.1				
1400 (2PE)	$CHCl_3$	1.7 ± 0.1	−0.71	16.5 ± 0.5	−0.29	233 ± 7

[a] τ_{S1} represents the S_1 lifetime, and τ_1 and τ_2 represent lifetimes of the first- and second-exponential rise/decay for the long-lived absorption band around 1510 cm^{-1}. [b] See ref 29 for detailed analyses of the S_1 lifetimes. [c] The excitation wavelength used for each data set. [d] Amplitudes are in arbitrary units, and a positive one represents a decay and a negative one a rise.

1.7 ps with 2PE in chloroform solution, which is also strongly dependent on solvent polarity.[29] The exponential fit parameters for the long-lived absorption bands around 1510 cm^{-1} for carotenoids **I** and **II** are summarized in Table 1 along with the S_1 lifetimes obtained via 1PE and 2PE.

Difference infrared spectra of **I** and **II** with 2PE show that the infrared spectra of long-lived species of both carotenoids are completely different from their ground-state infrared spectra and have a very strong $\nu_{C=C,sym}$ mode around 1510 cm^{-1} for both **I** and **II**.

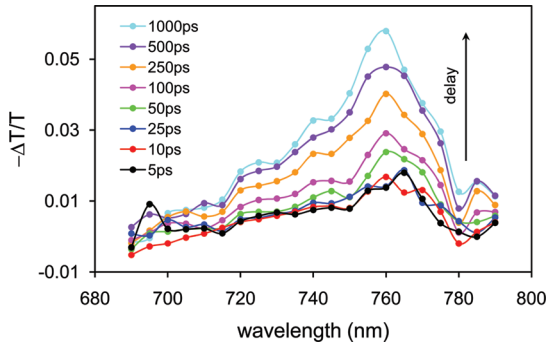

Figure 3. Transient absorption spectra of **I** in chloroform solution following 2PE at 1275 nm at selected time delays.

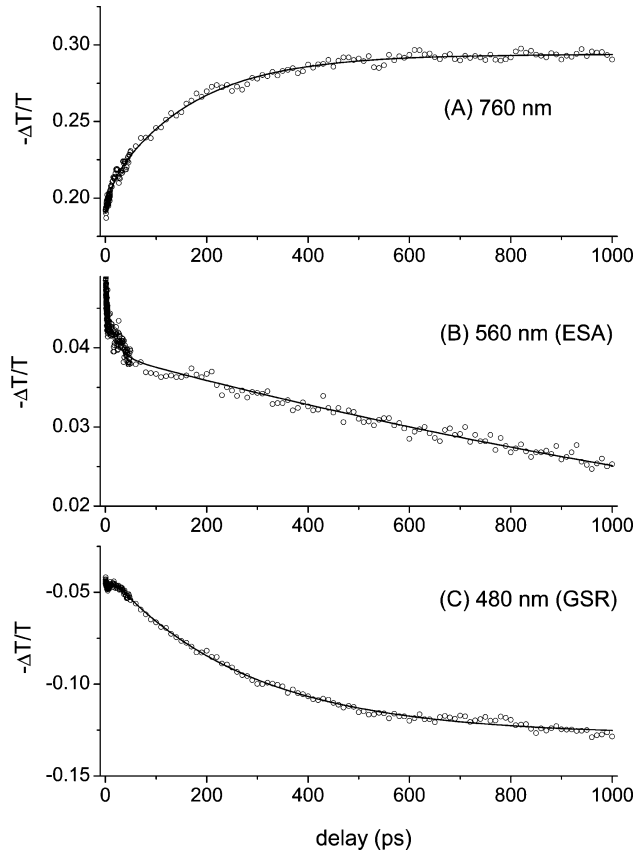

Figure 4. Kinetic traces (circles) and exponential fits (lines) for transient absorption of **I** in chloroform solution following 2PE at 1275 nm at probe wavelengths of (A) 760, (B) 560, and (C) 480 nm.

Transient Visible/Near-Infrared Absorption Spectroscopy of 8′-Apo-*β*-caroten-8′-al with 2PE. The transient absorption spectrum of **I** in chloroform was measured over the wavelength range 480−800 nm following 2PE at 1275 nm. Transient absorption spectra in the 690−790 nm region at selected time delays are shown in Figure 3. They show an absorption band centered at 760 nm which does not show decay by 1 ns delay. The kinetic trace for this band is plotted in Figure 4 in addition to those for the $S_1 \rightarrow S_N$ excited-state absorption (ESA) at 560 nm and the ground-state recovery (GSR) measured at 480 nm. The ESA band shows not only a decay component of the S_1 lifetime (∼18 ps) but also a much slower decay component with a ∼2.2 ns time constant. The fit of the GSR at 480 nm gives a very small decay component with 21.9 ps time constant (similar to the S_1 lifetime) and a strong rise component with a 270 ps time constant which is considered as an additional bleach signal and has not decayed by 1 ns.

Table 2. Exponential Fits for Transient Absorption Kinetic Traces of 8′-Apo-*β*-caroten-8′-al in Chloroform[a]

probe λ (nm)	a_1[b]	τ_1 (ps)	a_2[b]	τ_2 (ps)
480	0.10	21.9 ± 4.5	−1.00	270 ± 6
500	0.17	38.6 ± 6.6	−1.00	270 ± 10
520	0.06	13.3 ± 4.1	−1.00	302 ± 6
560	0.14	18.0 ± 1.8	0.86	2243 ± 53
650	−0.28	20.1 ± 5.3	−0.72	249 ± 23
720	0.27	6.4 ± 2.5	−1.00	200 ± 20
760	−0.14	11.0 ± 2.1	−0.86	166 ± 5

[a] Two-photon excitation (2PE) at 1275 nm was used for transient absorption measurements. [b] Amplitudes are in arbitrary units, and a positive one represents a decay and a negative one a rise.

The long-lived rise component is observed over the whole 600−800 nm probe wavelength range. The exponential fit of the 760 nm band kinetic trace shows two rise components with 11.0 and 166 ps time constants, which are very similar to the time constants of 15.4 and 142 ps measured from the 1510 cm^{-1} infrared band of **I** with 2PE. The exponential fit parameters from the visible/near-infrared transient absorption measurements are summarized in Table 2.

Potential-Energy Surface of 8′-Apo-*β*-caroten-8′-al. There have been numerous studies of the ground-state potential-energy surfaces of carotenoids including *β*-carotene,[8,11−14] and it is well established that these molecules exhibit a number of different conformations along the *β*-ring rotation and the trans−cis isomerization in the conjugated polyene.[8,12,36,37] The *β*-ring rotation which changes the relative geometry of the cyclohexene ring with respect to the plane of polyene has been known to have many effects on the stability and vibrational spectrum of carotenoids.[8,11,12] The potential-energy profile of **I** at the B3LYP/6-31G(d) level for the rotation about the C_6-C_7 bond is shown in Figure 5A. In this energy profile along the $C_5=C_6-C_7=C_8$ torsion angle coordinate, the global minimum energy point corresponds to the fully optimized s-cis structure and all the energies are referenced to this structure. The remaining points (separated from each other by about 20°) correspond to constrained structures where the $C_5=C_6-C_7=C_8$ torsion angle was frozen and all of the remaining nuclear degrees of freedom were fully optimized. The resulting potential-energy profile gives three minima separated by three transition points. Each of these geometries were fully optimized and characterized by harmonic frequency analysis.

The global minimum s-cis structure shows a torsional angle of 45.8°, which is consistent with the values for other carotenoids from X-ray crystallographic studies (∼42° for *β*-carotene[38] and ∼43° for canthaxanthin[39]) and DFT simulations (44.3° for zeaxanthin[8] and 39.4° for astaxanthin[14]). The next lowest energy minimum, which can be seen in Figure 5A at −47.6°, corresponds to the s-cis′ conformer, the second form of the s-cis conformer, and has an energy of 1.21 kJ/mol above the s-cis value. The final minimum energy point in Figure 5A, at a torsion angle of 169.2°, corresponds to the s-trans form of the structure which has an energy of 5.3 kJ/mol above s-cis.

(36) Bernardi, F.; Garavelli, M.; Olivucci, M.; Robb, M. A. *Mol. Phys.* **1997**, *92*, 359.
(37) Koyama, Y.; Takatsuka, I.; Nakata, M.; Tasumi, M. *J. Raman Spectrosc.* **1988**, *19*, 37.
(38) Senge, M. O.; Hope, H.; Smith, K. M. *Z. Naturforsch. C* **1992**, *47*, 474.
(39) Bart, J. C. J.; Macgilla, Ch. *Acta Crystallogr.* **1968**, *B24*, 1587.

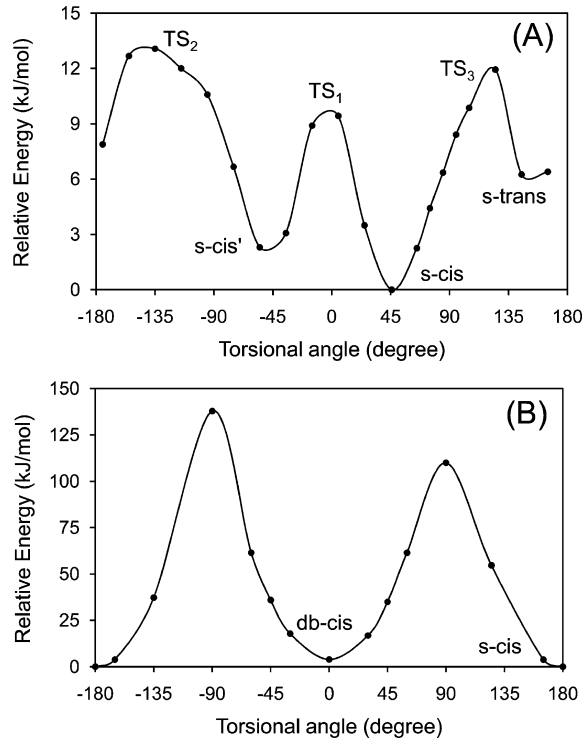

Figure 5. Potential-energy profile of **I** along the torsional angle coordinates of (A) $C_5{=}C_6{-}C_7{=}C_8$ and (B) $C_{12}{-}C_{13}{=}C_{14}{-}C_{15}$ at the B3LYP/6-31G(d) level. The energies (in kJ/mol) are relative to the s-cis conformation.

The energy difference between these conformers are quite similar to the values for zeaxanthin: 4.1 kJ/mol for the s-trans and 1.2 kJ/mol for the s-cis′ conformer.[8] Harmonic analyses of these conformers resulted in no imaginary frequencies, and this is consistent with the study of Dreuw, where a very similar energetic profile was found for zeaxanthin.[8] All of the minimized energy structures possess a similar bond length alternation pattern in which the single/double-bond length alternation is strongest at the terminal ends of the conjugated chain and becomes weaker toward the center. This is consistent with other DFT studies of carotenoids.[8,40]

The three transition structures of TS_1 (−3.9°, 9.8 kJ/mol), TS_2 (−146.5°, 13.0 kJ/mol), and TS_3 (124.9°, 11.4 kJ/mol) were found after the full optimizations. The harmonic frequency analyses show three imaginary frequencies of 66.2*i*, 26.0*i*, and 30.0*i* cm^{-1} for TS_1, TS_2, and TS_3, respectively, which correspond to the torsional modes that link the two conformers next to each transition structure. The rotational barriers (9.8−13.0 kJ/mol) for the s-cis conformer of **I** make the β-ring rotation slow at room temperature, where k*T* is about 2.5 kJ/mol. However, when the ground state is reached from the excited states, substantial population could be produced in the s-trans conformer.

We now consider trans−cis isomerization around the C=C bonds in the polyene backbone.[36,37] There are many possible isomers around the C=C bonds, but we chose the $C_{13}{=}C_{14}$ bond in the center of the backbone of **I** which can change the geometry of the molecule most drastically and thus, we expect, also strongly alter the vibrational spectrum. This is supported by an experimental study which showed that central-bent β-carotene has several distinguishable vibrational bands from those of stretched or terminal-bent β-carotene.[37] Figure 5B displays the torsion angle profile about the $C_{13}{=}C_{14}$ bond of carotenoid **I** at the B3LYP/6-31G(d) level where all other degrees of freedom other than the torsional angle are fully optimized. The energy scale in this figure is referenced to the s-cis conformer, which is the global minimum of the molecule and has the trans geometry at the $C_{13}{=}C_{14}$ bond. The db-cis conformer with a cis geometry at the $C_{13}{=}C_{14}$ bond has an energy of 3.9 kJ/mol above s-cis after full optimization, and a harmonic frequency analysis gives no imaginary frequencies.

One can immediately see in Figure 5B that the rotational barrier about this double bond is about 110 kJ/mol (9200 cm^{-1}), which is almost 2/3 of the S_1 energy level of **I**. If the system undergoes a trans to cis isomerization about this double bond while in the S_1 excited state and decays to the ground state in the db-cis geometry, the ground-state population may in fact stay trapped in the db-cis conformer for some time.

Simulated Infrared Spectra. We used the B3LYP/6-31G(d) level of DFT to calculate the frequencies and infrared strengths of the normal modes for s-cis, s-trans, and db-cis conformers of **I** and **II**. Simulated infrared spectra were generated by creating Gaussian functions from the normal modes in DFT simulations and by summing them up as

$$I(x) = \sum_{j}^{nm} I_j \exp\left[-\frac{(\nu_j^{sc} - x)^2}{\sigma^2}\right]$$

where $I(x)$ is the intensity of the simulated spectrum at position x along the frequency coordinate, I_j is the intensity, and ν_j^{sc} is the scaled frequency of the jth normal mode by a common scaling factor of 0.9613 for the B3LYP functional.[41] The width of the Gaussian, σ^2, was chosen so that the fwhm of each simulated infrared band is 15 cm^{-1} close to the experimental values in the ground-state infrared spectra for **I** and **II**.

Infrared spectra for the s-cis (global minimum), s-trans, and db-cis conformers of **I** predicted by the DFT simulations are shown in Figure 6A in addition to an FT-IR spectrum of **I** in chloroform solution. The infrared spectrum for the s-cis′ conformer is almost identical to the s-cis conformer and will not be discussed further. Comparing the simulated IR spectrum of the s-cis conformer with the FT-IR spectrum, we assign the vibrational modes of **I** in chloroform solution as (a) the symmetric C=C stretching mode ($\nu_{C=C,sym}$) along the backbone chain at 1524 cm^{-1}, (b) the asymmetric C=C stretching mode ($\nu_{C=C,asym}$) along the backbone chain at 1568 cm^{-1}, (c) the asymmetric C=C stretching mode which includes the cyclohexene ring stretching ($\nu_{C=C,asym+ring}$) at 1611 cm^{-1}, and (d) the C=O stretching mode ($\nu_{C=O}$) at 1669 cm^{-1}. There are some notable shortcomings of the simulated spectrum of the ground-state s-cis conformer of **I**. In the experimental spectrum the $\nu_{C=C,asym+ring}$ is somewhat stronger than the $\nu_{C=C,sym}$ but this is reversed in the calculated s-cis spectrum. The simulated spectra of all conformers do, however, produce a very intense $\nu_{C=O}$, consistent with the experimental spectrum.

The simulated spectra for the s-cis, s-trans, and db-cis conformers of **I** are quite similar to each other, but there is a notable difference in the symmetric stretching mode centered at 1520, 1515, and 1522/1537 cm^{-1} for the s-cis, s-trans, and db-cis conformers, respectively. The intensity of this mode increases for the s-trans conformer since it has a more linear

(40) Guo, J. D.; Luo, Y.; Himo, F. *Chem. Phys. Lett.* **2002**, *366*, 73.

(41) (a) Foresman, J. B.; Frisch, A. *Exploring Chemistry with Electronic Structure Methods*, 2nd ed.; Gaussian: Pittsburgh, PA, 1996. (b) Miller, T. M.; Van Doren, J. M.; Morris, R. A.; Viggiano, A. A. *Int. J. Mass Spectrom.* **2001**, *205*, 271.

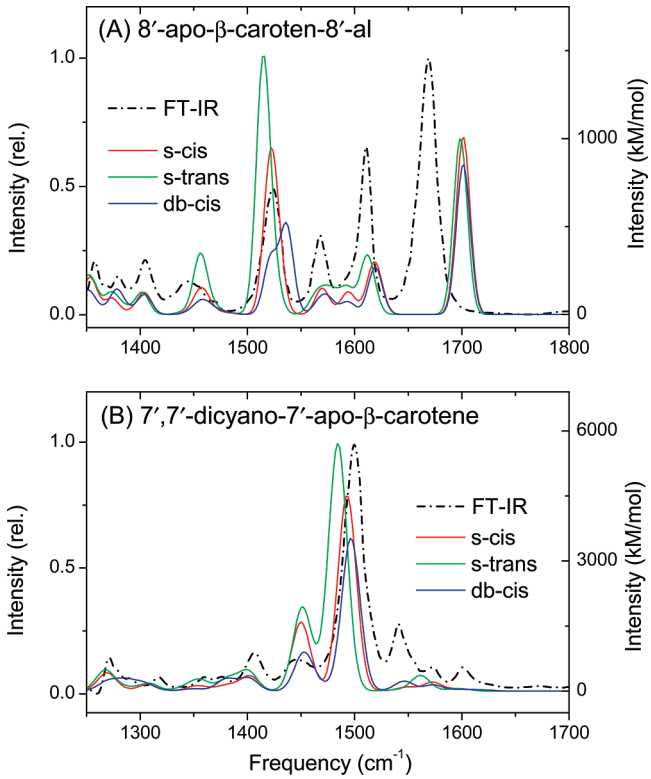

Figure 6. Simulated IR spectra for the optimized s-cis, s-trans, and db-cis conformers and an FT-IR spectrum in chloroform solution for (A) **I** and (B) **II**. Infrared intensities for the simulated spectra (in kM/mol) are shown in the right *y* axis.

structure than the s-cis conformer, and thus, the $\nu_{C=C,sym}$ can give rise to a bigger change in dipole moment. This $\nu_{C=C,sym}$ mode splits into two smaller peaks in the db-cis conformer due to the change in the molecular symmetry.

Figure 6B shows simulated infrared spectra for the s-cis (global minimum), s-trans, and db-cis conformers of **II** and an FT-IR spectrum of **II** in chloroform. By comparing the FT-IR and simulated spectra of **II**, we assign the major bands as (a) the symmetric C═C stretching ($\nu_{C=C,sym}$) mixed with CH_3 deformation bending ($\delta_{CH3,def}$) at 1444 cm^{-1}, (b) the symmetric C═C stretching ($\nu_{C=C,sym}$) at 1500 cm^{-1}, (c) the asymmetric C═C stretching modes ($\nu_{C=C,asym}$) at 1541 cm^{-1}, and (d) the asymmetric C═C stretching modes which are also delocalized into the cyclohexene ring ($\nu_{C=C,asym+ring}$) at 1573 and 1601 cm^{-1}. The DFT simulation of the s-cis conformer of **II** clearly gives the assignment of the $\nu_{C=C,sym}$ mode, but the relative intensities of other $\nu_{C=C}$ vibrations are quite different from the FT-IR spectrum. All vibrational frequencies and assignments of s-cis conformers of **I** and **II** are summarized in Table 3 with the experimental values from the FT-IR spectra in chloroform solution.

The simulated IR spectra of the s-trans and db-cis conformers of **I** and **II** are almost identical to the s-cis ground-state spectrum of each molecule as shown in Figure 6. Although there are significant changes in the molecular geometry and the dipole moment, none of these conformers show a very strong $\nu_{C=C,sym}$ around 1510 cm^{-1} of long-lived species.

Discussion

The transient infrared spectra of carotenoids **I** and **II** described in ref 29 and this work are consistent with these molecules having two noncommunicating minima on the S_1 potential surface: one reached via relaxation from S_2, and the second populated directly by two-photon absorption from the ground state. Furthermore, these two minima, which we label $S_{1,1PE}$ and $S_{1,2PE}$ for convenience, have different decay paths. $S_{1,1PE}$ decays directly to the ground state with no detectable intermediate aside from the hot ground state in the case of **II**. In the case of $S_{1,2PE}$, a long-lived state is formed detectable via both transient infrared spectroscopy and transient visible spectroscopy. In particular, the infrared spectrum in the region of $\nu_{C=C,sym}$ (~1510 cm^{-1}) is very different in the long-lived intermediate than in the ground state. Below we discuss various possible origins of this long-lived species.

Table 3. Vibrational Frequencies of 8′-Apo-β-caroten-8′-al and 7′,7′-Dicyano-7′-apo-β-carotene[a]

vibrational assignment	FT-IR[b]	simulation[c]
8′-Apo-β-caroten-8′-al (**I**)		
$\delta_{C=C-C} + \delta_{CHx(mixed)}$	1357	1353
$\delta_{CH3,def} + \delta_{CH,in-plane}$ (delocal.)	1380	1374
$\delta_{CH3,def} + \delta_{CH,in-plane}$ (local.)	1405	1404
$\delta_{CH3,def}$	1445	1457
$\nu_{C=C,sym}$	1524	1521
$\nu_{C=C,asym}$	1568	1569
$\nu_{C=C,asym+ring}$	1611	1596
		1618
$\nu_{C=O}$	1669	1701
7′,7′-Dicyano-7′-apo-β-carotene (**II**)		
$\delta_{CH,in-plane} + \delta_{CH2,wag}$	1271	1269
$\delta_{CH,in-plane}$	1317	1308
$\delta_{CH3,def} + \delta_{CH2,wag}$	~1360	1353
$\delta_{CH3,def}$	1407	1403
$\nu_{C=C,sym} + \delta_{CH3,def}$	1444	1450
$\nu_{C=C,sym}$	1500	1496
$\nu_{C=C,asym}$	1541	1549
$\nu_{C=C,asym+ring}$	1573	1572
$\nu_{C=C,asym+ring}$	1601	~1595
		1621

[a] All frequencies are in units of cm^{-1}. [b] An FT-IR spectrum in chloroform solution. [c] A simulated infrared spectrum of the s-cis conformer.

Triplet Formation. Perhaps the first explanation to consider is that the new spectral features arise from a triplet state. The $T_1 \rightarrow T_N$ absorption at 520 nm is well characterized, but we found negligible absorption in this region.[29]

Conformational Isomerization. Many conformations are possible for molecules **I** and **II**, and to test the possibility that long-lived conformational isomers are formed during relaxation of $S_{1,2PE}$ we used DFT to explore the infrared spectra of various conformers of **I** and **II**. However, as Figure 6 shows, the calculated infrared spectra of the s-cis′ (not shown, identical to that of s-cis) and s-trans conformers of **I** and **II** are almost identical to the s-cis ground-state spectrum. Similarly, the db-cis conformer (which would only be formed via an excited state as the barrier between it and the s-cis conformation is ~110 kJ/mol) has a very similar spectrum to the s-cis form. The only notable change in db-cis is that the $\nu_{C=C,sym}$ splits into 2 peaks for **I** and becomes weaker in both molecules as compared to s-cis. It thus seems unlikely that conformational isomerization provides the explanation for the long-lived species formed from $S_{1,2PE}$.

Soliton Pairs. Extended, conjugated linear polyenes can give rise to covalent and ionic excitons in the excited singlet states.[42] Early theoretical studies on long and infinite polyenes, by

Schulten and co-workers,[43] indicated the difficulty in modeling these types of excited-state systems accurately. Many years later, Garavelli et al. undertook a reaction path dynamics study on conjugated polyenes ($N = 3-6$) using a complete active space self-consistent field (CAS-SCF) and hybrid molecular mechanics-valence bond (MM-VB) theory.[44] These results showed the creation and annihilation dynamics of transient π-diradical species, also called a neutral soliton pair, which is formed via a passage through a conical intersection between the S_1 and S_0 states.[44] The soliton pair in the ground state forms a "kinked" structure, and surprisingly, this soliton pair can exist for a relatively long time (up to 1 ps; depending on the conjugation length). These diradicals are not restricted to a metastable minimum-energy state but are dynamically roaming over the ground-state potential-energy surface near the conical intersection. The diradicals can only annihilate with one another when the molecular geometry of the polyene backbone is favorable. In the case of conjugated molecules with chromophoric units, such as the carotenoids in this study, it is possible that the soliton pair may exist for significantly longer than 1 ps, especially in solution. The possibility of diradical formation must therefore be considered.

To explore whether the long-lived features of the difference infrared spectra could result from this soliton pair in the ground state, we calculated the IR spectrum of a hypothetical "kinked" structure of **I** in the ground state using DFT. The "kinked" structure is constructed by fixing two consecutive C=C−C bond angles to 90° ($C_{12}-C_{13}=C_{14}$ and $C_{13}=C_{14}-C_{15}$) and optimizing the remaining degrees of freedom, which only offers a "snapshot" of a huge conformational space. Unfortunately, dynamical calculations including excited states are not currently feasible for molecules of this size.

The carotenoid structure is only partially optimized, and the two imaginary frequencies of 246.2*i* and 73.6*i* cm^{-1} found in the harmonic frequency analysis correspond to twisting modes which drive the molecule from its "kinked" conformation to one of the s-cis conformations. While **I** is too large for a CAS-SCF conical intersection search, the similarity between the imaginary modes of the "kinked" structure of **I** and the conical intersection mode of the "kinked" polyenes[44] offers evidence that this "kinked" structure is likely to be in a region of the S_0 surface that corresponds to the lower surface of a conical intersection.

Figure 7A displays the simulated IR spectra of a "kinked" structure and the ground-state s-cis conformer of **I**. The vibrational modes of the "kinked" system are very different from the ground-state molecule. The intensity of $\nu_{C=C,sym}$ for a "kinked" conformer at 1522 cm^{-1} is 10 times smaller than that of the s-cis conformer because the distortions in the "kinked" geometry make the derivative of the dipole moment much smaller than that of the fully delocalized $\nu_{C=C,sym}$ of the s-cis conformer. This change contrasts to our finding of a strong increase in the intensity of the $\nu_{C=C,sym}$ as well as in the intensity of the $\nu_{C=C,asym}$ bleach at 1614 cm^{-1} of **I** following 2PE. The $\nu_{C=C,asym}$ of the "kinked" structure at 1606 cm^{-1} shows no major difference from that of the s-cis conformer. Thus, the long-lived absorption bands observed from the $S_{1,2PE}$ decay do not arise from a "kinked" structure formed in the electronic ground state after passing through a conical intersection with the S_1 state.

Neutral and Cation Radicals. A carotenoid radical could be the origin of the long-lived species formed from $S_{1,2PE}$. The formation of cation radicals upon photoexcitation have been reported by many groups.[18,21,22,45,46] For example, Skibsted and co-workers[18,21] used femtosecond excitation pulses (120−130 fs) to show that transient absorption bands of cation radicals (870−1000 nm) of β-carotene, zeaxanthin, astaxanthin, and all-*trans*-lycopene in chloroform solution are detected after 100−200 ps delay. The transient absorption band of cation radicals is formed from decay of the S_2 state in the case of β-carotene, zeaxanthin, and astaxanthin, while both the S_2 and S_1 states contribute in the case of all-*trans*-lycopene. In contrast, Polívka and co-workers[45] also used femtosecond pulses (~150 fs) to excite the S_2 state of zeaxanthin but did not observe a long-lived cation radical absorption band.

Vibrational (resonance Raman) spectra of cation radicals of **I** and **II** were recorded with a 752.6 nm excitation by Kispert and co-workers.[23] The $\nu_{C=C}$ modes of both carotenoids show red shifts of 40−46 cm^{-1} for **I** and 22−29 cm^{-1} for **II**, which is explained as a bond order decrease, similarly observed in the excited-state spectra. There is also a large change in the relative intensities of $\nu_{C=C,sym}$ and $\nu_{C=C,asym}$ upon oxidation: a very weak $\nu_{C=C,asym}$ in the neutral molecule becomes the most intense band in the cation radical, while the strong $\nu_{C=C,sym}$ in the neutral molecule becomes weaker in the cation radical.

Infrared spectra of the radicals of **I** and **II** in the fully optimized geometries were calculated with DFT at the B3LYP/6-31G(d) level in the electronic ground state. The spectrum of the cation radical of **I** is shown in Figure 7B along with the spectrum of the neutral molecule in the s-cis conformation. The cation radical spectrum of **I** has two major $\nu_{C=C}$, a very strong $\nu_{C=C,sym}$ (also delocalized into cyclohexene ring) at 1494 cm^{-1} and a weak $\nu_{C=C,asym}$ at 1522 cm^{-1}. The difference spectrum between the calculated cation and neutral forms of **I** is shown in Figure 7C. This difference spectrum is very similar to the experimental results using 2PE with a very strong band around 1510 cm^{-1} and a ground-state bleach of the $\nu_{C=C,asym+ring}$ around 1614 cm^{-1}. Such differences were not seen in the simulated spectra of any ground-state conformer. The dispersive pattern in the $\nu_{C=O}$ (1640−1680 cm^{-1} in experiment) is also shown at 1670−1730 cm^{-1} in the cation radical difference spectrum, although the relative intensity and frequency of $\nu_{C=O}$ are not accurate.

The formation of a neutral radical species by deprotonation from the cation radical at the C_4, C_5, C_9, and C_{13} positions has also been reported by Kispert and co-workers.[27,47] Recently, they measured the steady-state absorption spectra of neutral radicals of β-carotene in the molecular sieve $Cu^{(II)}$ MCM-41. The neutral radical with proton loss at the C_5 position shows the strongest absorption band (at 715 nm); the other neutral radicals deprotonated at C_4, C_9, and C_{13} show bands at 750, 675, and 535 nm, respectively. These absorption bands were

(42) (a) Soos, Z. G.; Ramasesha, S. *Phys. Rev. B* **1984**, *29*, 5410. (b) Tavan, P.; Schulten, K. *J. Chem. Phys.* **1986**, *85*, 6602. (c) Tavan, P.; Schulten, K. *J. Chem. Phys.* **1979**, *70*, 5407. (d) Schulten, K.; Ohmine, I.; Karplus, M. *J. Chem. Phys.* **1976**, *64*, 4422.
(43) Tavan, P.; Schulten, K. *Phys. Rev. B* **1987**, *36*, 4337.
(44) Garavelli, M.; Smith, B. R.; Bearpark, M. J.; Bernardi, F.; Olivucci, M.; Robb, M. A. *J. Am. Chem. Soc.* **2000**, *122*, 5568.
(45) Billsten, H. H.; Pan, J. X.; Sinha, S.; Pascher, T.; Sundstrom, V.; Polivka, T. *J. Phys. Chem. A* **2005**, *109*, 6852.
(46) Fujii, R.; Koyama, Y.; Mortensen, A.; Skibsted, L. H. *Chem. Phys. Lett.* **2000**, *326*, 33.
(47) (a) Gao, Y. L.; Webb, S.; Kispert, L. D. *J. Phys. Chem. B* **2003**, *107*, 13237. (b) Gao, Y. L.; Shinopoulos, K. E.; Tracewell, C. A.; Focsan, A. L.; Brudvig, G. W.; Kispert, L. D. *J. Phys. Chem. B* **2009**, *113*, 9901.

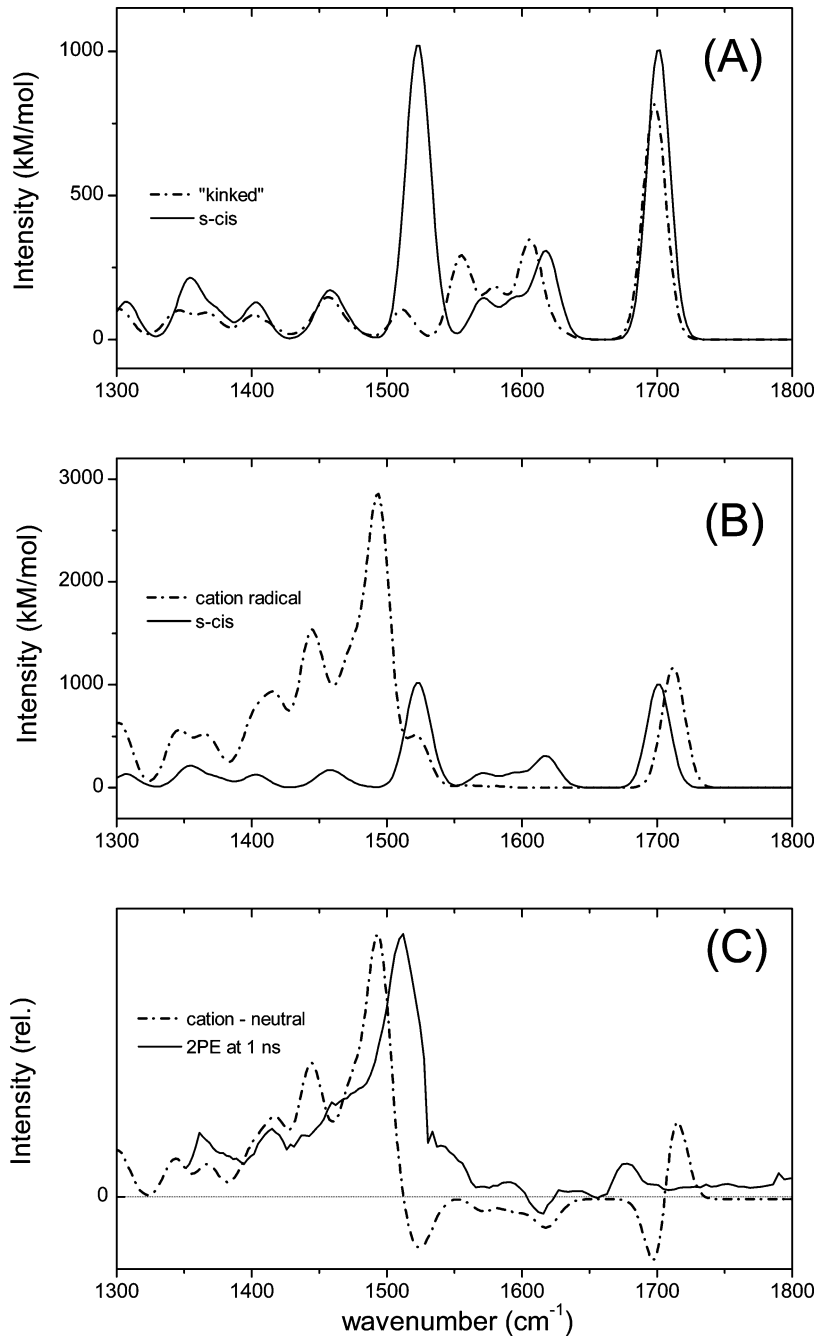

Figure 7. Simulated infrared spectra of a (A) "kinked" structure and the s-cis conformer of **I** and (B) cation radical and the s-cis conformer of **I**. (C) Simulated difference spectrum between a cation radical and the s-cis conformer (neutral) of **I** with the difference infrared spectrum of **I** in chloroform for 2PE at 1 ns delay.

assigned by TD-DFT simulations[27] in the gas phase with a scaling factor of 0.4 eV to accommodate the solvent effects. We applied the same DFT analysis on the neutral radicals at the C_4, C_5, C_9, C_{13}, $C_{13'}$, and $C_{9'}$ positions of both carotenoids; however, simulated spectra of the neutral radicals of **I** and **II** did not show significant differences from the ground-state molecule. In particular, a strong vibrational mode around 1510 cm^{-1} did not appear.

The transient absorption band at 760 nm of **I** formed from $S_{1,2PE}$ showed similar long-lived dynamics to the long-lived infrared absorption bands. This band does not correspond with the reported cation radical absorption band of **I** at 845 nm[23] or a measured value at 827 nm (created by chemical oxidation with I_2 and $FeCl_3$ in chloroform solution; data not shown). Attempts to observe an absorption signal at probe wavelengths of 800−900 nm from $S_{1,2PE}$ revealed nothing in addition to the 760 nm band described above. Neutral radicals which are deprotonated in the cyclohexene ring or dications of carotenoids (absorption band around 700 nm has been reported for several carotenoids[48]) have been reported to have absorption bands in the 700−800 nm range, so the transient absorption band at 760 nm could possibly arise from neutral radicals of **I** or a combination of cation and neutral radicals. However, this model

(48) (a) Jeevarajan, J. A.; Wei, C. C.; Jeevarajan, A. S.; Kispert, L. D. *J. Phys. Chem.* **1996**, *100*, 5637. (b) Krawczyk, S.; Olszowka, D. *Chem. Phys.* **2001**, *265*, 335.

does not provide an explanation for the additional ground-state bleach seen in Figure 4.

Nature of the Long-Lived Species. According to our DFT simulations the only species which generates a similar difference infrared spectrum to that observed in the experiments is the cation radical. However, we observed a significantly different visible spectrum centered at 760 nm from this species compared to those of the cation radical (827 or 845 nm). One clue to the nature of the long-lived species comes from the additional bleach of the ground-state absorption appearing with a rise time of ~270 ps, which suggests the participation of neighboring carotenoid molecules which are not initially excited by a laser pulse. The infrared spectra suggest that carotenoids **I** and **II** develop cationic character upon relaxation from $S_{1,2PE}$ perhaps via formation of a complex with a neighboring ground-state carotenoid molecule or solvent molecule.

Although the two-photon experiments are carried out at relatively high concentration ($\sim 10^{-3}$ M) the rate of formation of the long-lived species is much too fast to follow a diffusion-controlled process ($k_d = 1.33 \times 10^{10}$ M^{-1} s^{-1}) at this concentration. Thus, the complex would have to exist in the ground state, and the formation time reflects some structural rearrangement. The picture is further complicated by some recent results[49] in which we studied the effect of excess vibrational energy in S_2 following one-photon excitation. In ref 29 we excited near the minimum of S_2 of 8′-apo-β-caroten-8′-al at 490 nm. No long-lived species was observed even at a concentration of 4.8 mM. In the newer work,[49] we used 405 nm excitation corresponding to ~4000 cm^{-1} of excess vibrational energy. For this excitation wavelength, we find the same long-lived species (with a lower yield) as we observe for two-photon excitation even at concentrations as low as 75 μM. The strength of the 760 nm absorbance varies linearly with concentration over the range of 75−600 μM. These results suggest that a solvent complex with **I** and **II** formed only from a region of the ground-state potential surface accessible from vibrationally hot S_2 or the region of S_1 populated by two-photon excitation is a more likely explanation for the appearance of the cation-like spectrum.

This leaves us to explain the increasing ground-state bleach with a similar (270 ps), but not identical, rise time as the 760 nm band (166 ps) and the 1510 cm^{-1} IR band (142 ps) (all values for $CHCl_3$ solution). At present, we have no fully satisfactory explanation for the increasing ground-state bleach. If the two-photon excitation pulse, in addition to populating S_1, also populates a new region of the ground state directly (via a Raman process) and this region has a similar absorption spectrum to that of the original ground state, then the extent of the initial bleach of S_0 will be underestimated. The subsequent complex dynamics apparently involving multiple minima on the ground-state potential surface can then lead to a decrease in absorbance at the ground-state wavelength. An obvious way to check this proposal would be to carry out excitation at near-infrared wavelengths that are too long to allow two-photon excitation of S_1.

(49) Pang, Y.; Fleming, G. R. *Phys. Chem. Chem. Phys.* **2010**, submitted for publication.

Summary

We describe experimental evidence for the creation of long-lived species from carotenoids **I** and **II** resulting from 2PE-created populations of the S_1 state and theoretical modeling of various possible molecular species. The long-lived species is not created if S_1 is populated via one-photon excitation of S_2 and subsequent internal conversion. Infrared spectra of the long-lived species of **I** and **II** are similar to calculated spectra of cation radicals obtained via DFT at the B3LYP/6-31G(d) level. A transient absorption band centered at 760 nm is detected for **I**, and its dynamics is quite similar to those of the long-lived infrared absorption bands. We suggest that these spectral features correspond to a charge-transfer complex with a solvent molecule and that this state can only be formed from a region on the ground-state potential surface that is accessible from the region of S_1 populated by two-photon excitation but not by one-photon excitation near the origin of S_2 and subsequent internal conversion.

Acknowledgment. This research was funded by the NSF. We thank Prof. Lowell D. Kispert for his generous donation of the 7′,7′-dicyano-7′-apo-β-carotene molecule and many thoughtful discussions concerning our findings.

Supporting Information Available: Complete ref 34. This material is available free of charge via the Internet at http://pubs.acs.org.

JA908472Y